

# Classical methods in DIS and nuclear scattering at small $x$

Raju Venugopalan

*Physics Department, Brookhaven National Laboratory, Upton, NY 11973, USA*

## Abstract

In hadrons and nuclei at very small  $x$ , parton distributions saturate at a scale  $Q_s(x)$ . Since the occupation number is large, and  $Q_s(x) \gg \Lambda_{QCD}$ , classical weak coupling methods may be used to study this novel regime of non-linear classical fields in QCD. In these lectures, we apply these methods to compute structure functions in deeply inelastic scattering (DIS) and the energy density of gluons produced in high energy nuclear collisions.

# 1 Introduction

One of more interesting problems in perturbative QCD is the behaviour of parton distributions at small values of Bjorken  $x$ . In deeply inelastic scattering (DIS) for instance, for a fixed  $Q^2 \gg \Lambda_{QCD}^2$ , the operator product expansion (OPE) eventually breaks down at sufficiently small  $x$  [1]. Therefore at asymptotic energies, the conventional approaches towards computing observables based on the linear DGLAP [2] equations are no longer applicable. Even at current collider energies such as those of HERA, where the conventional wisdom is that the DGLAP equations successfully describe the data, there is reason to believe that effects due to large parton densities are not small. We may be at the threshold of a region where non-linear corrections to the evolution equations are large [3, 4].

In recent years, a non-OPE based effective field theory approach to small  $x$  physics has been developed by Lipatov and collaborators [5]. Their initial efforts resulted in an equation known popularly as the BFKL equation [6], which sums the leading logarithms of  $\alpha_S \log(1/x)$  in QCD. In marked contrast to the leading twist Altarelli-Parisi equations for instance, it sums all twist operators that contain the leading logarithms in  $x$ . The solutions to the BFKL equation predict a rapidly rising gluon density. Such a rapid rise in the gluon density is seen at HERA [7] but it can also arguably be accounted for by the next to leading order (NLO) DGLAP equations with appropriate choices of the initial parton densities [8].

Moreover, the next to leading logarithmic corrections to the BFKL equation computed in the above mentioned effective field theory (EFT) approach are *very* large [9]. Recently, as Gavin Salam has discussed in his lectures at this school [10], there has been considerable progress in understanding the source of these large corrections. The collinear enhancements from higher orders to the NLO BFKL kernel can be resummed, and this results in more stable estimates for the gluon anomalous dimensions, and for the hard pomeron. However, there are effects, not

included in such analyses, due to multiple pomeron exchange (non-linear QCD effects) that may become important at rapidity scales of interest. For instance, running coupling effects in the NLO BFKL equation become important at  $y \sim 1/\alpha_S^{5/3}$ . However, double (hard) pomeron effects will become important for  $y \sim 1/\alpha_S \log(1/\alpha_S)$ , a scale that is parametrically larger. How to systematically include such effects, which are enhanced by large parton densities, is an open question, and novel approaches need to be explored.

An alternative EFT approach to QCD at small  $x$  was put forward in a series of papers [11, 12, 13, 14, 15]. Our approach, is a Wilson renormalization group approach (RG) where the fields are those of the fundamental theory but the form of the action, at small  $x$ , is obtained by integrating out modes at higher values of  $x$ . This results in a set of non-linear renormalization group equations [15]. If the parton densities are not too high, the RG equations can be linearized, and have been shown to agree identically with the BFKL and small  $x$  DGLAP equations [14]. There is much effort underway to explore and make quantitative predictions for the non-linear regime beyond [16].

In these lectures, we will apply the above EFT to discuss two problems:

- Deeply inelastic scattering at small values of Bjorken  $x$  [18],
- high energy hadronic collisions [19, 20, 21].

Both are problems which appear extremely difficult to address in an OPE based analysis. They simplify in the regime where  $x$  is small and momentum transfers are large because, a) the gluon field at small  $x$  can be treated classically, and b) weak coupling methods apply. Why is this so? The reasons for these to apply have been discussed at length by Larry McLerran in his lectures [22] so we will be brief here.

At small  $x$ , one can define a scale  $\mu^2$  which measures the density of gluons per

unit transverse area. One has

$$\mu^2 = \frac{1}{\sigma} \frac{dN}{dy} \tag{1}$$

where  $\sigma$  is the hadronic or nuclear cross section of interest. Here  $y = y_0 - \ln(1/x)$ , and  $y_0$  is an arbitrarily chosen constant. When this scale satisfies the condition  $\mu \gg \alpha_S \mu \gg \Lambda_{QCD}$ , the occupation number of gluons in the hadron is large—thereby justifying the use of classical methods. Also, the intrinsic momentum  $p_t \sim \alpha_S \mu$  is large. Thus the gluon dynamics, while nonperturbative, is both semiclassical and weakly coupled.

Let us now discuss the classical field approach to small  $x$  DIS. The gluon field, being bosonic, has to be treated non-perturbatively. This is analogous to the strong field limit used in Coulomb problems. Fermions, on the other hand, do not develop a large expectation value and may be treated perturbatively. In DIS, to lowest order in  $\alpha_S$ , the gluon distribution function is determined by knowing the fermionic propagator in the classical gluon background field. In general, this propagator must be determined to all orders in the classical gluon field as the field is strong. This can be done due to the simple structure of the background field.

We will derive analytic expressions for the current–current correlator in deeply inelastic scattering by summing a particular class of all twist operators. These, we argue, give the dominant contribution at small  $x$ . At high  $Q^2$ , they reduce to the well known expressions for the leading twist structure functions [28]. For light quarks at high  $Q^2$ , it can be shown explicitly that the classical field analysis reproduces the DGLAP evolution equations for the quark distributions at small  $x$  [18]. The power of the technique we use to analyze the problem of DIS at small  $x$  is that, unlike the OPE, it does not rely on a twist expansion.

A similar point can be made about the classical approach to high energy hadronic scattering. At very high energies, the dominant contribution to particle production is from the interaction of the classical “Weizsäcker–Williams” (WW)

gluon fields of the two hadrons or nuclei. To lowest order, the picture is that of QCD Bremsstrahlung [43]. Soft gluons can be emitted from the valence quark/hard gluon lines, or from the  $2 \rightarrow 1$  diagram of two virtual gluons fusing to produce a hard gluon. At small  $x$ , in the Fock–Schwinger gauge ( $x^+ A^- + x^- A^+ = 0$ ) the latter WW contribution is the dominant one. The Weizsäcker–Williams contribution agrees with the QCD Bremsstrahlung result at small  $x$  [42, 41, 44, 45, 46].

It is essential to consider the full non-perturbative approach for the following reasons. Firstly, the classical gluon radiation computed perturbatively is infrared singular, and has to be cut-off at some scale  $k_t \sim \alpha_S \mu$ . This problem also arises in mini-jet calculations where at high energies results are shown to be rather sensitive to the cut-off [47]. Secondly, the non-perturbative approach is crucial to a study of the space-time evolution of the system. In particular, the possible thermalization of the system, as well as the relevant time scales for thermalization, are strongly influenced by the non-linearities that arise in the non-perturbative approach [48].

In these lectures, we will discuss results from real time simulations of the full, non-perturbative, evolution of classical non-Abelian WW fields. The fields are generated by sources of color charge  $\rho^\pm$  (representing the valence partons in each of the hadrons or nuclei) moving along the two light cones. For each  $\rho$  configuration, one solves Hamilton’s equation numerically to obtain the real time behavior of the gauge fields in the forward light cone. The Hamiltonian is the Kogut–Susskind Hamiltonian in 2+1-dimensions coupled to an adjoint scalar field. The initial conditions for the evolution are provided by the non-Abelian Weizsäcker–Williams fields for the nuclei before the collisions.

To compute observables, one has to average over all the  $\rho$  configurations in each of the two nuclei. In general, these are averaged with a statistical weight  $\exp[-F[\rho]]$ , where  $F[\rho]$  is a functional over the color charge density  $\rho$  of the higher  $x$  modes. The functional  $F[\rho]$  obeys the non-linear renormalization group equation that was mentioned in the preceding discussion. If one considers collisions of large

nuclei, the weight simplifies to a Gaussian one, and one can replace

$$F[\rho^\pm] \longrightarrow \int d^2x_t \int_y^{y_{frag}^\pm} dy' \frac{1}{\mu^2(y')} \text{Tr} \left( (\rho^\pm)^2 \right), \quad (2)$$

where  $y_{frag}^\pm$  are the rapidities corresponding to the fragmentation regions of the two nuclei.

Our approach is limited because it is classical. However, if the effective action approach captures the essential physics of the small  $x$  modes of interest, then in the spirit of the Wilson renormalization group, quantum information from the large  $x$  modes (above the rapidity of interest) is contained in the parameter  $\mu^2$  discussed above, which grows rapidly as one goes to smaller  $x$ 's. In principle, this information can be included in the classical lattice simulations.

The plan of these lectures is as follows. We will begin in section 2 by reviewing the effective action for the small  $x$  modes in QCD. We also discuss the classical saddle point solutions of this effective action. In section 3, we will discuss how one computes quark production in the classical gluon background field. At small  $x$ , this gives the dominant contribution to the structure functions measured in deeply inelastic scattering. Structure functions are computed in section 4. At high  $Q^2$ , our results reproduce the small  $x$  DGLAP results. For smaller values of  $Q^2$ , for Gaussian sources, one obtains the Glauber result for the structure functions in agreement with previous derivations in the nuclear rest frame. Subsequent sections concern gluon production in high energy scattering of (in particular) large nuclei. The classical approach to the two-nucleus problem is discussed in section 5. It is very hard to solve for the non-perturbative dynamics analytically. It has not yet been done. Instead, we derive a numerical algorithm which captures the essential physics of the two-nucleus problem. Results from our numerical simulations are discussed in section 6. Section 7 summarizes the material contained in the lectures and outlines directions of future research.

## 2 Effective Field Theory for Small $x$ Partons in QCD

In the infinite momentum frame (IMF)  $P^+ \rightarrow \infty$ , the effective action for the soft modes of the gluon field with longitudinal momenta  $k^+ \ll P^+$  (or equivalently  $x \equiv k^+/P^+ \ll 1$ ) can be written in light cone gauge  $A^+ = 0$  as

$$S_{eff} = - \int d^4x \frac{1}{4} G_{\mu\nu}^a G^{\mu\nu,a} + \frac{i}{N_c} \int d^2x_t dx^- \rho^a(x_t, x^-) \text{Tr} (\tau^a W_{-\infty, \infty}[A^-](x^-, x_t)) + i \int d^2x_t dx^- F[\rho^a(x_t, x^-)]. \quad (3)$$

Above,  $G_{\mu\nu}^a$  is the gluon field strength tensor,  $\tau^a$  are the  $SU(N_c)$  matrices in the adjoint representation and  $W$  is the path ordered exponential in the  $x^+$  direction in the adjoint representation of  $SU(N_c)$ ,

$$W_{-\infty, \infty}[A^-](x^-, x_t) = P \exp \left[ -ig \int dx^+ A_a^-(x^-, x_t) \tau^a \right]. \quad (4)$$

The action is a gauge invariant form [14] of the action that was proposed in Ref. [11]. One can write an alternative gauge invariant form of the action but the results are the same for the problem of interest.

The effective action considered here is valid in a limited range of  $P^+ \ll \Lambda^+$ , where  $\Lambda^+$  is an ultraviolet cutoff in the plus component of the momentum. The degrees of freedom at higher values of  $P^+$  have been integrated out. Their effect is to generate the second and third terms in the action. The first term is the usual field strength piece of the QCD action and describes the dynamics of the wee partons. The second term is the coupling of the wee partons to the hard color charges at higher rapidities, with  $x$  values corresponding to values of  $P^+ \geq \Lambda^+$ . When expanded to first order in  $A^-$ , this term gives the familiar  $J \cdot A$  coupling for Abelian classical fields. The last term in the effective action is imaginary. It can be thought of as a statistical weight resulting from integrating out the higher rapidity modes in the original QCD action. Expectation values of gluonic operators  $O(A)$

are then defined as

$$\langle O(A) \rangle = \frac{\int [d\rho] \exp(-F[\rho]) \int [dA] O(A) \exp(iS[\rho, A])}{\int [d\rho] \exp(-F[\rho]) \int [dA] \exp(iS[\rho, A])}, \quad (5)$$

where  $S[\rho, A]$  corresponds to the first two terms in Eq. 3.

In the IMF, only the  $J^+$  component of the current is large (the other components being suppressed by  $1/P^+$ ). The longer wavelength wee partons do not resolve the higher rapidity parton sources to within  $1/P^+$  and, for all practical purposes, one may write

$$\rho^a(x_t, x^-) \longrightarrow \rho^a(x_t) \delta(x^-). \quad (6)$$

In Ref. [11] a Gaussian form for the action

$$\int d^2x_t \frac{1}{2\mu^2} \rho^a \rho^a, \quad (7)$$

was proposed, where  $\mu^2$  was the average color charge squared per unit area of the sources at higher rapidities. For large nuclei  $A \gg 1$  it was shown that

$$\mu^2 = \frac{1}{\pi R^2} \frac{N_q}{2N_c} \sim A^{1/3} / 6 \text{ fm}^{-2}. \quad (8)$$

This result was independently confirmed in a model constructed in the nuclear rest frame [23]. If we include the contribution of gluons which have been integrated out by the renormalization group technique, one finds that [41]

$$\mu^2 = \frac{1}{\pi R^2} \left( \frac{N_q}{2N_c} + \frac{N_c N_g}{N_c^2 - 1} \right) \quad (9)$$

Here  $N_q$  is the total number of quarks with  $x$  above the cutoff;  $N_q = \sum_i \int_x^1 dx' q_i(x')$  where the sum is over different flavors, spins, quarks and antiquarks. For gluons, we also have  $N_g = \int_x^1 dx' g(x')$ . The value of  $\pi R^2$  is well defined for a large nucleus. For a smaller hadron, we must take it to be  $\sigma$ , the total cross section for hadronic interactions at an energy corresponding to the cutoff. This quantity will become better defined for a hadron in the renormalization group analysis.



The above equation for  $\mu^2$  is subtle because, implicitly, on the right hand side, there is a dependence on  $\mu$  through the structure functions themselves. This is the scale at which they must be evaluated. Calculating  $\mu$  therefore involves solving an implicit equation. Note that because the gluon distribution function rises rapidly at small  $x$ , the value of  $\mu$  grows as  $x$  decreases. At some critical  $x$ , the indications are that the parton distributions saturate. Thus there may be a critical line in the  $x$ - $Q^2$  plane corresponding to parton saturation. This is an important point and we will return to it later.

The Gaussian form of the functional  $F[\rho]$  is reasonable when the color charges at higher rapidity are uncorrelated and are random sources of color charge. This is true for instance in a very large nucleus. It is also true if we study the Fock space distribution functions or deep inelastic structure functions at a transverse momentum scale which is larger than an intrinsic scale set by  $\alpha_S \mu$ . In this equation  $\alpha_S$  is evaluated at the scale  $\mu$ . At smaller transverse momenta scales, one must do a complete renormalization group analysis to determine  $F[\rho]$ . For heavy quarks, in DIS, the Gaussian analysis should be adequate.

In Ref. [13], it was shown that a Wilson renormalization group procedure could be applied to derive a non-linear renormalization group equation for  $F[\rho]$ . In the limit of weak fields, the renormalization group equation can be linearized, and can be shown to be none other than the BFKL equation discussed previously. The fact that this limit can be obtained in a simple and elegant way suggests the power of this approach, and the importance of further studying the non-linear region of strong classical fields. We will not discuss the RG procedure here but will refer the reader to the relevant papers, and to Larry McLerran's lectures [22].

The effective action in Eq. 3 has a remarkable saddle point solution [11, 13, 23]. It is equivalent to solving the Yang-Mills equations

$$D_\mu G^{\mu\nu} = J^\nu \delta^{\nu+}, \quad (10)$$

in the presence of the source  $J^{+,a} = \rho^a(x_t, x^-)$ . Here we will allow the source to be smeared out in  $x^-$  as this is useful in the renormalization group analysis. It is also useful for intuitively understanding the nature of the field. One finds a solution where  $A^\pm = 0$  and

$$A^i = \frac{-1}{ig} V \partial^i V^\dagger, \quad (11)$$

( $i = 1, 2$ ) is a pure gauge field in the two transverse dimensions which satisfies the equation

$$D_i \frac{dA^i}{dy} = g\rho(y, x_\perp). \quad (12)$$

Here  $D_i$  is the covariant derivative  $\partial_i + V \partial_i V^\dagger$  and  $y = y_0 + \log(x^-/x_0^-)$  is the space-time rapidity and  $y_0$  is the space-time rapidity of the hard partons in the fragmentation region. At small  $x$ , we will use the space-time and momentum space notions of rapidity interchangeably [17]. The momentum space rapidity is defined to be  $y = y_0 - \ln(1/x)$ . The solution of the above equation is

$$A_\rho^i(x_t) = \frac{1}{ig} \left( P e^{ig \int_y^{y_0} dy' \frac{1}{\nabla_\perp^2} \rho(y', x_t)} \right) \nabla^i \left( P e^{ig \int_y^{y_0} dy' \frac{1}{\nabla_\perp^2} \rho(y', x_t)} \right)^\dagger. \quad (13)$$

The classical nuclear gluon distribution function is computed by averaging over the product of the classical fields in Eq. 13 at two space-time points with the weight  $F[\rho]$  [11]. For a Gaussian source, one obtains

$$\frac{dN}{d^2x_t} = \frac{1}{2\pi\alpha_S} \frac{C_F}{x_t^2} \left( 1 - \exp \left( -\frac{\alpha_S \pi^2}{2\sigma C_F} x_t^2 x G \left( x, \frac{1}{x_t^2} \right) \right) \right), \quad (14)$$

where  $C_F$  is the Casimir in the fundamental representation and  $\sigma$  is the nuclear cross-section<sup>1</sup>. For large  $x_t$  (but smaller than  $1/\Lambda_{QCD}$ , the distribution falls like a power law  $1/x_t^2$ —and has a  $1/\alpha_S$  dependence! For very small  $x_t$ , the behavior is the

<sup>1</sup> Above, we have re-written the expression for the gluon distribution in Ref. [13], using the leading log gluon distribution to replace  $\mu^2$  and  $\log(x_t \Lambda_{QCD})$  with the gluon distribution  $xG(x, \frac{1}{x_t^2})$  at the scale  $1/x_t^2$ .

perturbative distribution  $\log(x_t \Lambda_{QCD})$ . The scale which determines the cross-over from a logarithmic to a power law distribution is, following Mueller's notation [24], the saturation scale  $Q_s$ . Setting  $x_t = 1/Q_s$  and the argument of the exponential above to unity, one obtains the relation,

$$Q_s^2 = \frac{\alpha_S \pi^2}{2\sigma} \frac{1}{C_F} x G(x, Q_s^2), \quad (15)$$

which, for a particular  $x$ , can be solved self-consistently to determine  $Q_s$ .

Because of the sharp cut-off in co-ordinate space, the momentum space distribution is not well defined. A smooth Fourier transform has been defined, on physical grounds, by Lam and Mahlon by requiring that the charge in light cone gauge  $\int d^2 x_t \rho(x_t)$  vanish [25] for each  $\rho$  configuration.

### 3 Quark production in the classical gluon background field

In this section, we will compute the correlator of electromagnetic currents in the classical gluon background field. In deeply inelastic electroproduction, the hadron tensor can be expressed in terms of the forward Compton scattering amplitude  $T_{\mu\nu}$  by the relation [26]

$$\begin{aligned} W^{\mu\nu}(q^2, P \cdot q) &= 2Disc T^{\mu\nu}(q^2, P \cdot q) \equiv \frac{1}{2\pi} \text{Im} \int d^4 x \exp(iq \cdot x) \\ &\times \langle P | T(J^\mu(x) J^\nu(0)) | P \rangle, \end{aligned} \quad (16)$$

where ‘‘T’’ denotes time ordered product,  $J^\mu = \bar{\psi} \gamma^\mu \psi$  is the hadron electromagnetic current and ‘‘Disc’’ denotes the discontinuity of  $T_{\mu\nu}$  along its branch cuts in the variable  $P \cdot q$ . Also,  $q^2 \rightarrow \infty$  is the momentum transfer squared of the virtual photon<sup>2</sup> and  $P$  is the momentum of the target. In the IMF,  $P^+ \rightarrow \infty$  is the

---

<sup>2</sup> Note that in our metric convention, a space-like photon has  $q^2 = Q^2 > 0$ .

only large component of the momentum. The fermion state above is normalized as  $\langle P | P' \rangle = (2\pi)^3 E/m \delta^{(3)}(P - P')$  where  $m$  is the mass of the target hadron. This definition of  $W^{\mu\nu}$  and normalization of the state is traditional. In the end, all factors of  $m$  cancel from the definition of quantities of physical interest. (The normalization we will use in this paper for quark and lepton states will have  $E/m$  replaced by  $2P^+$ .)

We now generalize our definition of  $W^{\mu\nu}$  to a source which has a position dependence. We obtain

$$W^{\mu\nu}(q^2, P \cdot q) = \frac{1}{2\pi} \sigma \frac{P^+}{m} \text{Im} \int d^4x dX^- e^{iq \cdot x} \langle T (J^\mu(X^- + x/2) J^\nu(X^- - x/2)) \rangle . \quad (17)$$

To see this, first note that we can define  $\langle O \rangle = \langle P | O | P \rangle / \langle P | P \rangle$  where  $O$  is any operator. From the discussion above, the expectation value  $\langle P | P \rangle = (2\pi)^3 E/m \delta^{(3)}(0) = (2\pi)^3 E/m V$ . Here we shall take the spatial volume  $V$  to be  $\sigma$  times an integral over the longitudinal extent of the state. The variable  $X^-$  is a center of mass coordinate and  $x^-$  is the relative longitudinal position. The above definition of  $W^{\mu\nu}$  is Lorentz covariant. The integration over  $X^-$  is required since we must include all of the contributions from quarks at all  $X^-$  to the distribution function. In the external source language, the variable  $P^+$  can be taken to be the longitudinal momentum corresponding to the fragmentation region.

The expectation value is straightforward to compute in the limit where the gluon field is treated as a classical background field. If we write

$$\langle T(J^\mu(x) J^\nu(y)) \rangle = \langle T(\bar{\psi}(x) \gamma^\mu \psi(x) \bar{\psi}(y) \gamma^\nu \psi(y)) \rangle , \quad (18)$$

then when the background field is classical, we obtain

$$\langle T(J^\mu(x) J^\nu(y)) \rangle = \text{Tr}(\gamma^\mu S_A(x)) \text{Tr}(\gamma^\nu S_A(y)) + \text{Tr}(\gamma^\mu S_A(x, y) \gamma^\nu S_A(y, x)) . \quad (19)$$

In this expression,  $S_A(x, y)$  is the Green's function for the fermion field in the

external field  $A$

$$S_A(x, y) = -i \langle \psi(x) \bar{\psi}(y) \rangle_A . \quad (20)$$

The first term on the right hand side of Eq. 19 is a tadpole contribution without an imaginary part. It therefore does not contribute to  $W^{\mu\nu}$ . We find then that

$$\begin{aligned} W^{\mu\nu}(q^2, p \cdot q) &= \frac{1}{2\pi} \sigma \frac{P^+}{m} \text{Im} \int dX^- d^4x e^{iq \cdot x} \langle \text{Tr} \left( \gamma^\mu S_A(X^- + x/2, X^- - x/2) \right. \\ &\quad \left. \times \gamma^\nu S_A(X^- - x/2, X^- + x/2) \right) \rangle . \end{aligned} \quad (21)$$

The expression we derived above for  $W^{\mu\nu}$  is entirely general and makes no reference to the operator product expansion. In particular, it is relevant at the small  $x$  values and moderate  $q^2$  where the operator product expansion is not reliable [1]. At sufficiently high  $q^2$  though (and for massless quarks) it should agree with the usual leading twist computation of the structure functions.

We can derive an expression for the sea quark Fock distribution in terms of the propagator in light cone quantization [27]. One obtains

$$\frac{dN}{d^3k} = \frac{2i}{(2\pi)^3} \int d^3x d^3y e^{-ik \cdot (x-y)} \text{Tr} [\gamma^+ S_A(x, y)] \quad (22)$$

where the fermion propagator  $S_A(x, y)$  is defined as in Eq. 20. In a nice pedagogical paper, (see Ref. [28] and references within), Jaffe has shown that the Fock space distribution function can be simply related to the *leading twist* structure function  $F_2$  by the relation

$$F_2(x, Q^2) = \int_0^{Q^2} dk_t^2 x \frac{dN}{dk_t^2 dx} . \quad (23)$$

Actually, Jaffe's expression is defined as the sum of the quark and anti-quark distributions. At small  $x$ , these are identical and the resulting factor of 2 is already included in our definition of the light cone quark distribution function. At high  $q^2$ , our general (all twist) result for  $F_2$  agrees with the leading twist result derived using Eq. 23 [18].

Clearly, to compute  $W^{\mu\nu}$ , we first need to compute the fermion Green's function in the classical background field. The field strength carried by these classical gluons is highly singular, being peaked about the source (corresponding to the parton current at  $x$  values larger than those in the field) localized at  $x^- = 0$ . Away from the source, the field strengths are zero and the gluon fields are pure gauges on both sides of  $x^- = 0$  (see Eq. 11). The fermion wavefunction is obtained by solving the Dirac equation in the background field on either side of the source and matching the solutions across the discontinuity at  $x^- = 0$ . Once the eigenfunctions are known, the fermion propagator can be constructed, in the standard fashion, by writing

$$S(x, y) = \int \frac{d^4q}{(2\pi)^4} \frac{1}{q^2 + M^2 - i\varepsilon} \sum_{pol} \psi_q(x) \bar{\psi}_q(y), \quad (24)$$

after identifying  $q^+ = (q_t^2 + M^2 - \lambda)/2q^-$ . We will not discuss the details of the derivation here but refer the interested reader to Ref. [18].

Define

$$G(x_t, x^-) = \theta(-x^-) + \theta(x^-)V(x_t), \quad (25)$$

a gauge transformation matrix that transforms the gluon field at hand to a singular field with the only non-zero component,  $A'^\mu = \delta^{\mu+}\alpha(x_t)$ . Our result then is that the fermion propagator in the background field has the form [29, 18]

$$S_A(x, y) = G(x)S_0(x-y)G^\dagger(y) - i \int d^4z G(x) \left\{ \theta(x^-)\theta(-y^-)(V^\dagger(z_t) - 1) - \theta(-x^-)\theta(y^-)(V(z_t) - 1) \right\} G^\dagger(y)S_0(x-z)\gamma^- \delta(z^-)S_0(z-y). \quad (26)$$

with the free fermion Green's function

$$S_0(x-y) = \int \frac{d^4q}{(2\pi)^4} e^{iq \cdot (x-y)} \frac{(M - \not{q})}{q^2 + M^2 - i\varepsilon}. \quad (27)$$

Recall that  $V(x_t)$  is the gauge transformation matrix in the fundamental representation and that the classical solution  $A^i = V(x_t)\partial^i V^\dagger(x_t)/(-ig)$ . This very simple form of the propagator is useful in the manipulations below.

In fact, since the current-current correlation function is explicitly gauge invariant, we may use the singular gauge form of the propagator [30, 31] for computing the current-current correlation function

$$S_A^{sing}(x, y) = S_0(x - y) - i \int d^4 z \left\{ \theta(x^-) \theta(-y^-) (V^\dagger(z_t) - 1) - \theta(-x^-) \theta(y^-) (V(z_t) - 1) \right\} S_0(x - z) \gamma^- \delta(z^-) S_0(z - y). \quad (28)$$

A diagrammatic representation of the form of the propagator above is shown in Fig. 1 In the expressions below for  $W^{\mu\nu}$  we will drop the superscript *sing* and simply use the singular gauge expression for the propagator.



Figure 1: Diagrammatic representation of the propagator in Eq. 48.

Our result for the fermion propagator in the classical background field was obtained for a  $\delta$ -function source in the  $x^-$  direction. This assumption was motivated by the observation that small  $x$  modes with wavelengths greater than  $1/P^+$  perceive a source which is a  $\delta$ -function in  $x^-$ . The propagator above can also be derived for the general case where the source has a dependence on  $x^-$ . The gauge transforms above are transformed from  $V(x_t) \rightarrow V(x_t, x^-)$ , to path ordered exponentials, where  $V(x_t, x^-)$  is given by Eq. 13. Our result for the propagator is obtained as a smooth

limit of  $\Delta x^- = 1/xP^+ \gg x^- (= 1/P^+)$ . Therefore our form for the propagator is the correct one provided we interpret the  $\theta$ -functions and  $\delta$ -functions in  $x^-$  to be so only for distances of interest greater than  $1/P^+$ , the scale of the classical source.

We are now in a position to calculate the current–current correlator. This calculation is accurate to lowest order in  $\alpha_S$  but to all orders in  $\alpha_S\mu$ . Before we go ahead with the computation, we will discuss briefly the averaging procedure over the labels of color charges at rapidities higher than those of interest. This is required if we are to compute gauge invariant observables.

If we average the Green’s function in Eq. 26 over all possible values of the color labels corresponding to the partons at higher rapidities, we can employ the following definitions for future reference. Defining

$$\frac{1}{N_c} \langle \text{Tr} \left( V(x_t) V^\dagger(y_t) \right) \rangle_{\rho} = \gamma(x_t - y_t), \quad (29)$$

we see that  $\gamma(0) = 1$ , which follows from the unitarity of the matrices  $V$ . Now defining the Fourier transform<sup>3</sup>

$$\tilde{\gamma}(p_t) = \int d^2x_t e^{-ip_t x_t} [\gamma(x_t) - 1], \quad (30)$$

we have the sum rule

$$\int \frac{d^2p_t}{(2\pi)^2} \tilde{\gamma}(p_t) = 0. \quad (31)$$

The function  $\tilde{\gamma}(p_t)$  will appear frequently in our future discussions and as we shall see, can be related to the gluon density at small  $x$ .

We will now use the fermion Green’s function in Eq. 26 to derive an explicit result for the hadronic tensor  $W^{\mu\nu}$ . In the following section, we will compute the structure functions  $F_1$  and  $F_2$ . As previously, we define

$$W^{\mu\nu}(q, P, X^-) = \text{Im} \int d^4z e^{iq \cdot z} \langle T(J^\mu(X^- + \frac{z}{2}) J^\nu(X^- - \frac{z}{2})) \rangle, \quad (32)$$

---

<sup>3</sup>We define the Fourier transform in this way because it corresponds to only the connected pieces in the correlator.



where ‘‘Imaginary’’ stands for the discontinuity in  $q^-$ . Then

$$W^{\mu\nu}(q, P) = \frac{1}{2\pi} \sigma \frac{P^+}{m} \int dX^- W^{\mu\nu}(q, P, X^-) \equiv \frac{1}{2\pi} \sigma P^+ \text{Im} \int dX^- \int d^4z e^{iq \cdot z} \\ \times \text{Tr} \left( S_{A_{cl}} \left( X^- + \frac{z}{2}, X^- - \frac{z}{2} \right) \gamma^\nu S_{A_{cl}} \left( X^- - \frac{z}{2}, X^- + \frac{z}{2} \right) \gamma^\mu \right). \quad (33)$$

The only terms in the propagator that contribute to the above are the  $\theta(\pm x^-)\theta(\mp y^-)$  pieces. Using our representation for the propagator in Eq. 28, after considerable manipulations, we can write  $W^{\mu\nu}$  as

$$W^{\mu\nu}(q, P) = \frac{\sigma P^+ N_c}{2\pi m} \text{Im} \int \frac{d^4p}{(2\pi)^4} \frac{d^2k_t}{(2\pi)^2} \frac{dk^+}{(2\pi)} \tilde{\gamma}(k_t) \\ \times \text{Tr} \left\{ \frac{(M - \not{p}')\gamma^-(M - \not{l}')\gamma^\mu(M - \not{l}')\gamma^-(M - \not{p}')\gamma^\nu}{(p^2 + M^2 - i\varepsilon)(l^2 + M^2 - i\varepsilon)(l'^2 + M^2 - i\varepsilon)(p'^2 + M^2 - i\varepsilon)} \right\}, \quad (34)$$

where  $l = p - k$ ,  $l' = l - q$ ,  $p' = p - q$  and  $k^- = 0$ . Correspondingly, we can write  $W^{\mu\nu}$  as the imaginary part of the diagram shown in Fig. 2.

For the DIS case,  $q^2 > 0$  (see footnote 1), we can cut the above diagram only in the two ways shown in Fig. 3 (the diagram where both insertions from the external field are on the same side of the cut is forbidden by the kinematics).

Also interestingly, the contribution to  $W^{\mu\nu}$  can be represented solely by the diagram in Fig. 4 and not, as is usually the case, from the sum of this diagram and the standard box diagram. This is because in our representation of the propagator multiple insertions from the external field on a quark line can be summarized into a single insertion. Eq. 28 makes this point clear.

Applying the Landau–Cutkosky rule, shifting  $p \rightarrow p + k$ , and changing variables appropriately, Eq. 34 can be written as

$$W^{\mu\nu}(q, P) = \frac{\sigma P^+ N_c}{2\pi m} \int \frac{d^4p}{(2\pi)^4} \frac{d^2k_t}{(2\pi)^2} \frac{dk^+}{(2\pi)} \tilde{\gamma}(k_t) M^{\mu\nu} \theta(p^+ + k^+) \theta(-p^+) \\ \times (2\pi)^2 \delta((p + k)^2 + M^2) \delta((p - q)^2 + M^2) \frac{1}{p^2 + M^2} \frac{1}{(p + k - q)^2 + M^2}, \quad (35)$$

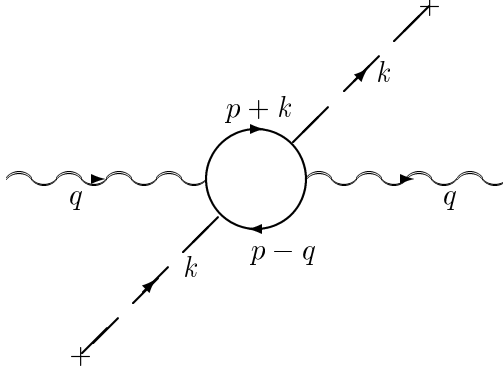


Figure 2: Polarization tensor with arbitrary number of insertions from the classical background field. Wavy lines are photon lines, the solid circle denotes the fermion loop and the dashed lines are the insertions from the background field (see Fig. 1). The imaginary part of this diagram gives  $W^{\mu\nu}$ .

where above the trace is represented by <sup>4</sup>

$$M^{\mu\nu} = \text{Tr} \left\{ (M - \not{p}' - \not{k}') \gamma^- (M - \not{p}') \gamma^\mu (M - \not{p}' + \not{q}') \gamma^- (M - \not{p}' - \not{k}' + \not{q}') \gamma^\nu + \mu \leftrightarrow \nu \right\}. \quad (36)$$

In Ref. [18], the integral over  $p^-$  in Eq. 34 was performed before the  $p^+$  integral. Here, we instead perform the  $p^+$  integral first. Further, defining  $z = p^-/q^-$ , we note that the  $\theta$ -function and  $\delta$ -function constraints in Eq. 34 restrict  $0 < z < 1$ .

<sup>4</sup>Kinematic note: the observant reader will notice we have put  $q^+ = 0$  here. Since we are working in the infinite momentum frame, the hadron has only one large momentum component,  $P^+$ . The rest are put to zero. For the photon, we choose a left moving frame such that  $q^0 = |q^z|$  and  $q^+ = 0$ . Then,  $q^2 = q_t^2 > 0$ ,  $P \cdot q = -P^+ q^-$  and  $x_{Bj} = -q^2/(2P \cdot q) \equiv q_t^2/(2P^+ q^-)$ . Since in the infinite momentum frame  $0 < x_{Bj} < 1$ , this gives  $q^- > 0$ .

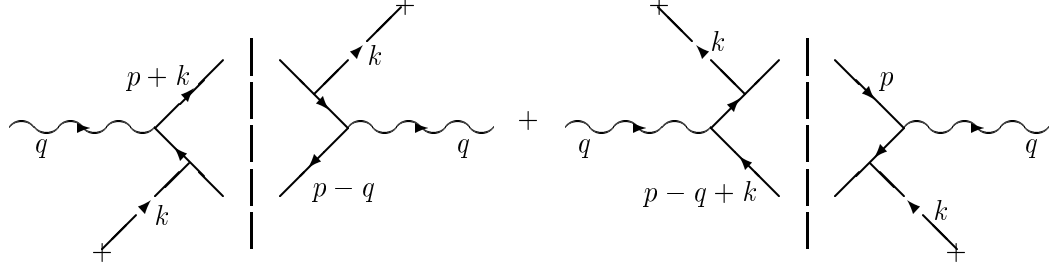


Figure 3: Cut diagrams corresponding to the imaginary part of  $W^{\mu\nu}$ .

This simplifies the result in Ref. [18] considerably. Performing the  $p^+$  integral, one obtains

$$\begin{aligned}
W^{\mu\nu}(q, P) &= \frac{\sigma P^+ q^- N_c}{\pi^2 m} \frac{1}{(q^-)^2} \int_0^1 dz \int \frac{d^2 p_t}{(2\pi)^2} \frac{d^2 k_t}{(2\pi)^2} \tilde{\gamma}(k_t) \frac{M^{\mu\nu}}{16} \\
&\times \frac{1}{M_p^2 + z(1-z)q_t^2} \frac{1}{M_{p+k-q}^2 + z(1-z)q_t^2}, \tag{37}
\end{aligned}$$

where  $M_p^2 = p_t^2 + M^2$ . Similarly  $M_{p+k-q}^2 = (p_t + k_t - q_t)^2 + M^2$ . The above is the final result of this section, and will be used below in computing structure functions.

## 4 Structure Functions at Small $x$

The hadronic tensor  $W^{\mu\nu}$  can be decomposed in terms of the structure functions  $F_1$  and  $F_2$  as [26]

$$mW^{\mu\nu} = -\left(g^{\mu\nu} - \frac{q^\mu q^\nu}{q^2}\right) F_1 + \left(P^\mu - \frac{q^\mu (P \cdot q)}{q^2}\right) \left(P^\nu - \frac{q^\nu (P \cdot q)}{q^2}\right) \frac{F_2}{(P \cdot q)}, \tag{38}$$

where  $P^\mu$  is the four-momentum of the hadron or nucleus and  $P^2 = m^2 \approx 0$  ( $\ll q^2$ ). In the infinite momentum frame, we have  $P^+ \rightarrow \infty$  and  $P^-, P_t \approx 0$ .

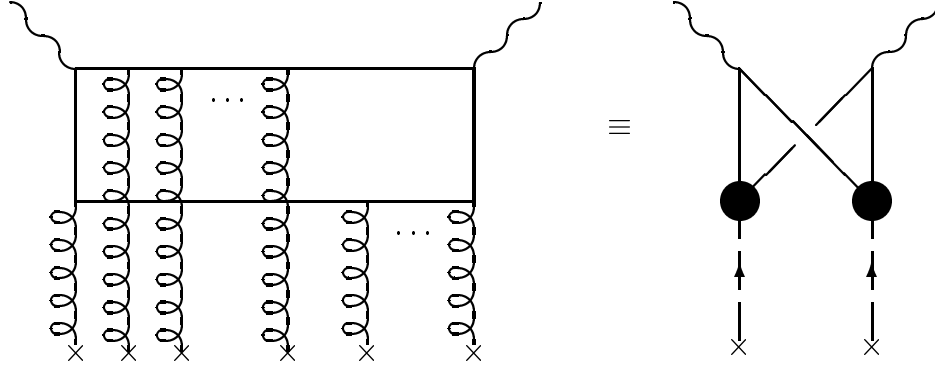


Figure 4: In the singular gauge representation for the propagator (see Eq. 28 and Fig. 1), the current–current correlator (imaginary part of LHS) is equivalent to the imaginary part of RHS.

The above equation can be inverted to obtain expressions for  $F_1$  and  $F_2$  in terms of components of  $W^{\mu\nu}$ . Since in our kinematics  $q^+ = 0$  (see footnote 3 for a kinematic note) we have

$$F_1 = \frac{F_2}{2x} + \left( \frac{q^2}{(q^-)^2} \right) W^{--} ; \quad \frac{1}{2x} F_2 = - \left( \frac{(q^-)^2}{q^2} \right) W^{++}. \quad (39)$$

It is useful to verify explicitly that our expression for  $W^{\mu\nu}$  derived in an external field can be written in the form of Eqn. 38. Recall that  $W^{\mu\nu}$  can be written in Lorentz covariant form by using the vector  $n^\mu = \delta^{\mu+}$ . Using  $n \cdot \gamma = -\gamma^-$  in Eqn. 34, we see that  $W^{\mu\nu}$  is a Lorentz covariant function of the only vectors in the problem— $q^\mu$  and  $n^\mu$ . Identifying  $n^\mu = P^\mu/P^+$  in Eqn. 38, we see that these forms are in complete agreement. Note that all factors of  $m$  disappear from  $F_1$  and  $F_2$  by the explicit forms of Eqns. 38 and 34.

We also see that the structure functions can only be functions of  $q^2$  and  $n \cdot q$  by Lorentz invariance. We can therefore take  $q^+ = 0$  for the purpose of computing

$F_1$  and  $F_2$ .

To compute  $W^{++}$  and  $W^{--}$ , we need to know the traces  $M^{++}$  and  $M^{--}$ , respectively in Eq. 37. We can compute them explicitly and the results can be represented compactly as

$$\frac{1}{16}M^{++} = \frac{1}{2} \left( M_p^2 M_{p+k-q}^2 + M_{p+k}^2 M_{p-q}^2 - q_t^2 k_t^2 \right), \quad (40)$$

and

$$M^{--} = 32(p^-)^2(p^- - q^-)^2. \quad (41)$$

From the relations above of  $F_1$  and  $F_2$  to  $W^{++}$  and  $W^{--}$ , we obtain from Eq. 37 the following general results for the structure functions for arbitrary values of  $Q^2$ ,  $M^2$  and the intrinsic scale  $\mu$ ,<sup>5</sup>

$$F_2 = \frac{Q^2 \sigma N_c}{2\pi^3} \int_0^1 dz \int_0^{\frac{1}{\Lambda_{QCD}}} dx_t x_t (1 - \gamma(x_t, y)) \\ \times \left[ K_0^2(x_t A) \left( 4z^2(1-z)^2 Q^2 + M^2 \right) + K_1^2(x_t A) A^2 \left( z^2 + (1-z)^2 \right) \right] \quad (42)$$

Here  $A^2 = Q^2 z(1-z) + M^2$  and  $K_{0,1}$  are the modified Bessel functions. For simplicity, we have ignored the impact parameter dependence of  $\gamma$  and replaced the integral over impact parameter by the transverse area  $\sigma$ . For the same reason, we ignore the sum over the charge squared of the quark flavors. Both of these must of course be included in numerical computations. The first (second) term in the bracket above is the probability for a longitudinally (transversely) polarized photon to split into a  $\bar{q}q$  pair. Ignoring target mass corrections which are negligible at small  $x$ ,

$$F_L = F_2 - 2xF_1 \\ \equiv \frac{Q^2 \sigma N_c}{\pi^3} \int_0^1 dz \int_0^{\frac{1}{\Lambda_{QCD}}} dx_t x_t (1 - \gamma(x_t, y)) z^2(1-z)^2 Q^2 K_0^2(x_t A). \quad (43)$$

---

<sup>5</sup>which is implicitly contained in the function  $\tilde{\gamma}(k_t)$  in Eq. 37.

For a Gaussian source (see Ref. [18] and footnote 1),

$$\gamma(x_t, y) = \exp\left(-\frac{\alpha_S \pi^2}{2\sigma N_c} x_t^2 x G\left(x, \frac{1}{x_t^2}\right)\right), \quad (44)$$

where the scale is set by the transverse separation  $x_t$  between the quark and the anti-quark.

The equation for  $F_2$  with the Gaussian source is the well known Glauber expression [32] usually derived in the rest frame of the nucleus. It is heartening to see that the formalism of Ref. [18] for structure functions in the infinite momentum frame reproduces it. For large  $Q^2$ , it reduces to the standard small  $x$  DGLAP expression<sup>6</sup> while at small  $Q^2$  it goes to zero as  $Q^2 \log(Q^2)$ . One then recovers, qualitatively, the shape of the famous Caldwell plot for  $dF_2/d\log(Q^2)$  measured at HERA [33]. Similar forms were used by several authors to understand the recent data [34].

One obtains from the above equation for  $F_2$ , in a manner analogous to Eq. 14, the quark saturation scale  $Q_s^q$  by replacing  $C_F \rightarrow C_A$  in Eq. 15. The relative size of the two saturation scales, glue to quark, is therefore determined simply by the ratio of the two Casimirs,  $C_A/C_F$ .

What about quantum corrections to the above quark and gluon distributions? At the one loop level, one gets  $\log(1/x)$  corrections to the Weizsacker–Williams distribution [35, 12, 24]. However, Mueller has argued recently that beyond the one loop level, the distribution has the same form as the as the above classical gluon distribution. What does change due to small  $x$  evolution is the  $x$  dependence of the saturation scale [24]. Recently, there have been detailed studies by Kovchegov, and by Levin and Tuchin, of parton evolution in the non-linear region [36, 37]. Their results appear to confirm the intuitive picture of Mueller.

As  $q^2 \rightarrow \infty$ , we find remarkably that the integral on the RHS of Eq. 43

---

<sup>6</sup>In Ref. [18], it was shown explicitly that our general expression for  $F_2$  formally reduces to the leading twist expression obtained from Eq. 22.

vanishes and it reduces to

$$F_1 = \frac{F_2}{2x}. \quad (45)$$

The above is the well known Callan–Gross relation. The reader may note above that the deviation from the Callan–Gross relation vanishes as a power law as  $q^2 \rightarrow \infty$ . On the other hand, it is well known in QCD [39, 40] that the violations of the Callan–Gross relation only disappear logarithmically as  $q^2 \rightarrow \infty$ . The apparent contradiction is resolved by one realizing that the logarithmic violations at large  $q^2$  in QCD come from diagrams where the sea quark emits a gluon (thereby violating Feynman’s parton model helicity argument). These diagrams are of higher order in our picture and are therefore not included. In fact, the deviations from the Callan–Gross relation of the sort discussed above (at small  $x$ ) should die off faster than logarithmically at very large  $q^2$  because for sufficiently large  $q^2$ , the violations of the Callan–Gross relation should come from precisely the diagrams not included here. At moderate  $q^2$  however, the contributions we have discussed above should be important.

## 5 The non–Abelian Weizsäcker–Williams approach to high energy nuclear collisions

In nuclear collisions at very high energies, the hard valence parton modes in each of the nuclei act as highly Lorentz contracted, static sources of color charge for the wee parton, Weizsäcker–Williams modes in the nuclei. The sources are described by the current

$$J^{\nu,a}(r_t) = \delta^{\nu+} g \rho_1^a(r_t) \delta(x^-) + \delta^{\nu-} g \rho_2^a(r_t) \delta(x^+), \quad (46)$$

where  $\rho_1$  ( $\rho_2$ ) correspond to the color charge densities of the hard modes in nucleus 1 (nucleus 2) respectively. The classical field of two nuclei is described by the solution

of the Yang–Mills equations in the presence of the light cone sources:

$$D_\mu F^{\mu\nu} = J^\nu, \quad (47)$$

Gluon distributions are simply related to the Fourier transform  $A_i^a(k_t)$  of the solution to the above equation by  $\langle A_i^a(k_t) A_i^a(k_t) \rangle_\rho$ . The averaging over the classical charge distributions is defined by

$$\langle O \rangle_\rho = \int d\rho_1 d\rho_2 O(\rho_1, \rho_2) \exp\left(-\int d^2r_t \frac{\text{Tr}[\rho_1^2(r_t) + \rho_2^2(r_t)]}{2\mu^2}\right), \quad (48)$$

and is performed independently for each nucleus with equal Gaussian weight  $\mu^2$ . Of course, this is only true for identical nuclei.

Before the nuclei collide ( $t < 0$ ), a solution of the equations of motion is

$$A^\pm = 0; \quad A^i = \theta(x^-)\theta(-x^+)\alpha_1^i(r_t) + \theta(x^+)\theta(-x^-)\alpha_2^i(r_t), \quad (49)$$

where  $\alpha_q^i(r_t)$  ( $q = 1, 2$  denote the labels of the nuclei) are pure gauge fields of the two nuclei before the collision and have the form described in Eq. 13. The above expression suggests that for  $t < 0$  the solution is simply the sum of two disconnected pure gauges.

For  $t > 0$  the solution is no longer pure gauge. Working in the Schwinger gauge  $A^\tau \equiv x^+ A^- + x^- A^+ = 0$  the authors of Ref. [42] found that with the ansatz

$$A^\pm = \pm x^\pm \alpha(\tau, r_t); \quad A^i = \alpha_\perp^i(\tau, r_t), \quad (50)$$

where  $\tau = \sqrt{2x^+x^-}$ , Eq. 47 could be written in the simpler form

$$\begin{aligned} \frac{1}{\tau^3} \partial_\tau \tau^3 \partial_\tau \alpha + [D_i, [D^i, \alpha]] &= 0, \\ \frac{1}{\tau} [D_i, \partial_\tau \alpha_\perp^i] + ig\tau [\alpha, \partial_\tau \alpha] &= 0, \\ \frac{1}{\tau} \partial_\tau \tau \partial_\tau \alpha_\perp^i - ig\tau^2 [\alpha, [D^i, \alpha]] - [D^j, F^{ji}] &= 0. \end{aligned} \quad (51)$$

The above equations of motion are independent of  $\eta$ —the gauge fields in the forward light cone are therefore only functions of  $\tau$  and  $r_t$  and are explicitly boost invariant.



This result follows from the assumption that the sources of color charge are delta functions on the light cone. Of course this is not true in general. However, we are interested in the region of central rapidity, about one unit of rapidity around  $\eta = 0$ . The boost invariance assumption should be Ok in this region. Also note that boost invariance is *not* assumed when solving for the fields of the nuclei before the collision.

The initial conditions for the fields  $\alpha(\tau, r_t)$  and  $\alpha_{\perp}^i$  at  $\tau = 0$  are obtained by matching the equations of motion (Eq. 47) at the point  $x^{\pm} = 0$  and along the boundaries  $x^+ = 0, x^- > 0$  and  $x^- = 0, x^+ > 0$ . Remarkably, there exist a set of non-singular initial conditions for the smooth evolution of the classical fields in the forward light cone. These can be written in terms of the fields of each of the nuclei before the collision ( $t < 0$ ) as follows,

$$\alpha_{\perp}^i|_{\tau=0} = \alpha_1^i + \alpha_2^i ; \quad \alpha|_{\tau=0} = \frac{ig}{2}[\alpha_1^i, \alpha_2^i]. \quad (52)$$

Gyulassy and McLerran have shown [41] that even when the fields  $\alpha_{1,2}^i$  before the collision are smeared out in rapidity to properly account for singular contact terms in the equations of motion the above boundary conditions remain unchanged. Further, the only condition on the derivatives of the fields that would lead to regular solutions are  $\partial_{\tau}\alpha|_{\tau=0}, \partial_{\tau}\alpha_{\perp}^i|_{\tau=0} = 0$ .

In Ref. [42], perturbative solutions (for small  $\rho$ ) were found to order  $\rho^2$  by expanding the initial conditions and the fields in powers  $\rho$  (or equivalently, in powers of  $\alpha_S\mu/k_t$ ) We will not discuss the details of the perturbative solution but wish to refer the reader to the original papers.

Perturbatively, at late times, the fields in the forward light cone can be expanded out in plane waves. The energy distribution in a transverse box of size  $R$  and longitudinal extent  $dz$  can be computed by summing over the energy of the modes in the box with the occupation number of the modes given by the mode functions

$a_i(k_t)$ . We have then

$$\frac{dE}{dyd^2k_t} = \frac{1}{(2\pi)^2} \sum_{i,b} |a_i^b(k_t)|^2. \quad (53)$$

The multiplicity distribution of classical gluons is defined as  $dE/dyd^2k_t/\omega$ . After performing the averaging over the Gaussian sources, the number distribution of classical gluons is

$$\frac{dN}{dyd^2k_t} = \pi R^2 \frac{2g^6\mu^4}{(2\pi)^4} \frac{N_c(N_c^2 - 1)}{k_t^4} L(k_t, \lambda), \quad (54)$$

where  $L(k_t, \lambda)$  is an infrared divergent function at the scale  $\lambda$ . This result agrees with the quantum bremsstrahlung formula of Gunion and Bertsch [43] and with several later works [44, 41, 45, 46].

The function  $L(k_t, \lambda)$  arises from long range color correlations that are cut-off either by a nuclear form factor (as in Refs. [43, 44]), by dynamical screening effects [49, 50] or in the classical Yang–Mills case of Ref. [42], non-linearities that become large at the scale  $k_t \sim \alpha_S\mu$ . In the classical case,  $L(k_t, \lambda) = \log(k_t^2/\lambda^2)$ , where  $\lambda = \alpha_S\mu$ . The formalism used in all these derivations breaks down at small momenta and one cannot distinguish between the different parametrizations of the nuclear form factors. However, at sufficiently high energies, the behaviour of  $L(k_t, \lambda)$  in the infrared is given by higher order (in  $\alpha_S\mu/k_t$ ) non-linear terms in the classical effective theory. We hope to understand in the near future how non-perturbative effects in the classical effective theory dynamically change the gluon distributions at small transverse momenta.

While the Yang–Mills equations discussed above can be solved perturbatively in the limit  $\alpha_S\mu \ll k_t$ , it is unlikely that a simple analytical solution exists for Eq. 47 in general. The classical solutions have to be determined numerically for  $t > 0$ . The straightforward procedure would be to discretize Eq. 47 but it will be more convenient for our purposes to construct the lattice Hamiltonian and obtain the lattice equations of motion from Hamilton’s equations.

Let us first consider the continuum Hamiltonian [19]. In the appropriate  $(\tau, \eta, x_t)$  co-ordinates, the metric is diagonal with  $g^{\tau\tau} = -g^{xx} = -g^{yy} = 1$  and  $g^{\eta\eta} = -1/\tau^2$ .

After a little algebra, the Hamiltonian can be written as [51]

$$H = \tau \int d\eta d^2 r_t \left\{ \frac{1}{2} p^\eta p^\eta + \frac{1}{2\tau^2} p^r p^r + \frac{1}{2\tau^2} F_{\eta r} F_{\eta r} + \frac{1}{4} F_{xy} F_{xy} + j^\eta A_\eta + j^r A_r \right\}. \quad (55)$$

Here we have adopted the gauge  $A^\tau = 0$ . Also,  $p^\eta = \frac{1}{\tau} \partial_\tau A_\eta$  and  $p^r = \tau \partial_\tau A_r$  are the conjugate momenta.

Consider the field strength  $F_{\eta r}$  in the above Hamiltonian. If we assume approximate boost invariance, or

$$A_r(\tau, \eta, \vec{r}_t) \approx A_r(\tau, \vec{r}_t); \quad A_\eta(\tau, \eta, \vec{r}_t) \approx \Phi(\tau, \vec{r}_t), \quad (56)$$

we obtain

$$F_{\eta r}^a = -D_r \Phi^a, \quad (57)$$

where  $D_r = \partial_r - igA_r$  is the covariant derivative. Further, if we express  $j^{\eta,r}$  in terms of the  $j^\pm$  defined in Eq. 46 we obtain the enormously simplifying result that  $j^{\eta,r} = 0$  for  $\tau > 0$ . Due to boost invariance, our effective Hamiltonian acts in 2+1-dimensions. It is possible to relax this assumption, but then the numerical simulations are more complicated.

We now consider the equivalent lattice action and Hamiltonian. The appropriate action is derived starting from the Minkowski Wilson action in the discretized 4-space and taking the naive continuum limit in the longitudinal and time directions. Replacing  $a^2 \sum_{zt}$  with  $\int dzdt$  in the Minkowski Wilson action, we then have for the 2+1-dimensional action

$$S = \int dzdt \sum_{\perp} \left[ \frac{1}{2N_c} \text{Tr} F_{zt}^2 + \frac{1}{N_c} \Re \text{Tr} (M_{t\perp} - M_{z\perp}) - \left( 1 - \frac{1}{N_c} \Re \text{Tr} U_{\perp} \right) \right], \quad (58)$$

where

$$M_{t,jn} \equiv \frac{1}{2} (A_{t,j}^2 + A_{t,j+n}^2) - U_{j,n} \left[ \frac{1}{2} \partial_t^2 U_{j,n}^\dagger + i (A_{t,j+n} \partial_t U_{j,n}^\dagger - \partial_t U_{j,n}^\dagger A_{t,j}) + A_{t,j+n} U_{j,n}^\dagger A_{t,j} \right], \quad (59)$$

and similarly for  $M_{z,jn}$ .

The equation of motion for a field is obtained by varying  $S$  with respect to that field. For the longitudinal fields  $A_{t,z}$  the variation has the usual meaning of a partial derivative. For transverse link matrices  $U_{\perp}$  the variation amounts to a covariant derivative. Just as in the continuum case, the lattice initial conditions can be determined from the lattice action in Eq. 58. One obtains the lattice equations of motion in the four light cone regions and then determines non-singular initial conditions by matching at  $\tau = 0$  the coefficients of the most singular terms in the equations of motion.

On the lattice, the initial conditions are the constraints on the longitudinal gauge potential  $A^{\pm}$  and the transverse link matrices  $U_{\perp}$  at  $\tau = 0$ . The longitudinal gauge potentials can be written as in the continuum case (see Eq. 50) as

$$A^{\pm} = \pm x^{\pm} \theta(x^+) \theta(x^-) \alpha(\tau, x_t). \quad (60)$$

The transverse link matrices are, for each nucleus, pure gauges before the collision. This fact is reflected by writing

$$U_{\perp} = \theta(-x^+) \theta(-x^-) I + \theta(x^+) \theta(x^-) U(\tau) + \theta(-x^+) \theta(x^-) U_1 + \theta(x^+) \theta(-x^-) U_2, \quad (61)$$

where  $U_{1,2}$  are pure gauge. The pure gauges are defined on the lattice as follows. To each lattice site  $j$  we assign two  $SU(N_c)$  matrices  $V_{1,j}$  and  $V_{2,j}$ . Each of these two defines a pure gauge lattice gauge configuration with the link variables  $U_{j,\hat{n}}^q = V_{q,j} V_{q,j+n}^{\dagger}$  where  $q = 1, 2$  labels the two nuclei. As in the continuum, the gauge transformation matrices  $V_{q,j}$  are determined by the color charge distribution  $\rho_{q,j}$  of the nuclei, normally distributed with the standard deviation  $\mu^2$ :

$$P[\rho_q] \propto \exp \left( -\frac{1}{2\mu^2} \sum_j \rho_{q,j}^2 \right). \quad (62)$$

Parametrizing  $V_{q,j}$  as  $\exp(i\Lambda_j^q)$  with Hermitean traceless  $\Lambda_j^q$ , we then obtain  $\Lambda_j^q$  by

solving the lattice Poisson equation

$$\Delta_L \Lambda_j^q \equiv \sum_n \left( \Lambda_{j+n}^q + \Lambda_{j-n}^q - 2\Lambda_j^q \right) = \rho_{q,j}. \quad (63)$$

It is easy to verify that the correct continuum solution (Eqs. 49 and 50) for the transverse fields  $A_\perp$  is recovered by taking the formal continuum limit of Eq. 61.

The equation of motion for  $U_\perp$ , contains, upon substitution of  $U_\perp$  from (61) and  $A^\pm$  from (60), singular terms containing the product  $\delta(x^-)\delta(x^+)$ . These originate in the double-derivative contributions  $\Re \text{Tr} U_\perp^\dagger \partial_+ \partial_- U_\perp$  in the action, when both derivative operators act on the step functions. Since the coefficient in front of  $\delta(x^+)\delta(x^-)$  must vanish in order to satisfy the equation of motion, a matching relation between  $U_\perp$  and  $U_{1,2}$  is obtained.

$$\text{Tr} \sigma_\gamma \left[ (U_1 + U_2)(I + U_\perp^\dagger) - \text{h.c.} \right] = 0. \quad (64)$$

Our result is that  $(U_1 + U_2)(I + U_\perp^\dagger)$  should have no anti-Hermitean traceless part. Note that this condition has the correct formal continuum limit: writing  $U_{1,2}$  as  $\exp(ia_\perp \alpha_{1,2})$  and  $U_\perp$  as  $\exp(ia_\perp \alpha_\perp)$ , we have, for small  $a_\perp$ , the result  $\alpha_\perp = \alpha_1 + \alpha_2$ , as required. The above condition in Eq. (64) can easily be resolved in the SU(2) case but we have not yet found a simple closed form expression for  $N_c > 2$ . For SU(2), one obtains for the initial condition

$$U_\perp = (U_1 + U_2)(U_1^\dagger + U_2^\dagger)^{-1}. \quad (65)$$

For the  $A_-$  field, the singularities arise from the Abelian part of the  $F_{+-}^2$  term in the action whose variation with respect to  $A^{+, \gamma}$  gives

$$\frac{1}{N_c} \text{Tr} \sigma_\gamma \partial_+ (\partial_- A_+ - \partial_+ A_-). \quad (66)$$

Its most singular part is  $\alpha_\gamma \theta(x^-)\delta(x^+)$ . Varying the  $\pm, \perp$  terms (Eq. 59) in the action (Eq. 58) with respect to  $A_j^{+, \gamma}$  and selecting the contributions containing derivatives, one obtains eventually the result

$$\alpha_\gamma = \frac{i}{4N_c} \sum_n \text{Tr} \sigma_\gamma \left( [(U_1 - U_2)(U^\dagger - I) - \text{h.c.}]_{j,n} - [(U^\dagger - I)(U_1 - U_2) - \text{h.c.}]_{j-n,n} \right). \quad (67)$$

It is easily seen that the above equation has the correct formal continuum limit. Writing again  $U_{1,2}$  as  $\exp(ia_\perp\alpha_{1,2})$  and  $U$  as  $\exp(ia_\perp\alpha_\perp)$ , one finds in the limit of smooth fields,  $\alpha = i\sum_n[\alpha_1, \alpha_2]_n$ , as required.

The lattice action is essential to obtain the initial conditions for the evolution of fields in the forward light cone. For the evolution, we need the lattice Hamiltonian. It is obtained by performing a Legendre transform of Eq. 58 following the standard Kogut-Susskind procedure [52]. The analog of the Kogut-Susskind Hamiltonian here is

$$\begin{aligned}
H_L &= \frac{1}{2\tau} \sum_{l \equiv (j, \hat{n})} E_l^a E_l^a + \tau \sum_{\square} \left( 1 - \frac{1}{2} \text{Tr} U_{\square} \right), \\
&+ \frac{1}{4\tau} \sum_{j, \hat{n}} \text{Tr} \left( \Phi_j - U_{j, \hat{n}} \Phi_{j+\hat{n}} U_{j, \hat{n}}^\dagger \right)^2 + \frac{\tau}{4} \sum_j \text{Tr} p_j^2, \tag{68}
\end{aligned}$$

where  $E_l$  are generators of right covariant derivatives on the group and  $U_{j, \hat{n}}$  is a component of the usual SU(2) matrices corresponding to a link from the site  $j$  in the direction  $\hat{n}$ . The first two terms correspond to the contributions to the Hamiltonian from the chromoelectric and chromomagnetic field strengths respectively. In the last equation  $\Phi \equiv \Phi^a \sigma^a$  is the adjoint scalar field with its conjugate momentum  $p \equiv p^a \sigma^a$ .

Lattice equations of motion follow directly from  $H_L$  of Eq. 68. For any dynamical variable  $v$  with no explicit time dependence  $\dot{v} = \{H_L, v\}$ , where  $\dot{v}$  is the derivative with respect to  $\tau$ , and  $\{\}$  denote Poisson brackets. We take  $E_l$ ,  $U_l$ ,  $p_j$ , and  $\Phi_j$  as independent dynamical variables, whose only nonvanishing Poisson brackets are

$$\{p_i^a, \Phi_j^b\} = \delta_{ij} \delta_{ab}; \quad \{E_l^a, U_m\} = -i\delta_{lm} U_l \sigma^a; \quad \{E_l^a, E_m^b\} = 2\delta_{lm} \epsilon_{abc} E_l^c$$

(no summing of repeated indices). The equations of motion are consistent with a set of local constraints (Gauss' laws).

The results of this section can be summarized as follows. The four independent dynamical variables are  $E_l$ ,  $U_\perp$ ,  $p_j$  and  $\Phi_j$ . Their evolution in  $\tau$  after the nuclear

collision is determined by Hamilton's equations above and their values at the initial time  $\tau = 0$  are specified by the following initial conditions:

$$\begin{aligned} U_{\perp}|_{\tau=0} &= (U_1 + U_2)(U_1^{\dagger} + U_2^{\dagger})^{-1} ; E_l|_{\tau=0} = 0 . \\ p_j|_{\tau=0} &= 2\alpha ; \Phi_j = 0 , \end{aligned} \tag{69}$$

where  $U_{\perp}$  and  $\alpha$  are given by Eq. 65 and Eq. 67 respectively.

## 6 Results for gluon production in high energy nuclear collisions

In this section we will discuss recent results for the energy density  $\varepsilon$  as a function of the proper time  $\tau$  [21]. Work on computing number distributions is in progress and will be reported at a later date [53]. In an earlier work, we confirmed that, in weak coupling, the results from our numerical simulations agreed with lattice perturbation theory [20].

The computation of energy densities on the lattice is straightforward. Our main result is contained in Eq. 70. To obtain this result, we compute the Hamiltonian density on the lattice for each  $\rho^{\pm}$ , and then take the Gaussian average (with the weight  $\mu^2$ ) over between 40  $\rho$  trajectories for the larger lattices and 160  $\rho$  trajectories for the smallest ones.

In our numerical simulations, all the relevant physical information is contained in  $g^2\mu$  and  $L$ , and in their dimensionless product  $g^2\mu L$  [54]. The strong coupling constant  $g$  depends on the hard scale of interest; from Eq. 9, we see that  $\mu$  depends on the nuclear size, the center of mass energy, and the hard scale of interest;  $L^2$  is the transverse area of the nucleus. Assuming  $g = 2$  (or  $\alpha_S = 1/\pi$ ),  $\mu = 0.5$  GeV (1.0 GeV) for RHIC (LHC), and  $L = 11.6$  fm for  $Au$ -nuclei, we find  $g^2\mu L \approx 120$  for RHIC and  $\approx 240$  for LHC. (The latter number would be smaller for a smaller

value of  $g$  at the typical LHC momentum scale.) As will be discussed later, these values of  $g^2\mu L$  correspond to a region in which one expects large non-perturbative contributions from a sum to all orders in  $Q_s \sim 6\alpha_S\mu$ , even if  $\alpha_S \ll 1$ . (Recall the definition of the saturation scale in Eq. 15.) Deviations from lattice perturbation theory, as a function of increasing  $g^2\mu L$ , were observed in our earlier work [20].

We shall now discuss some of the results from our numerical simulations. In Fig. 5, we plot  $\varepsilon\tau/(g^2\mu)^3$ , as a function of  $g^2\mu\tau$ , in dimensionless units, for the smallest, largest, and an intermediate value in the range of  $g^2\mu L$ 's studied. The

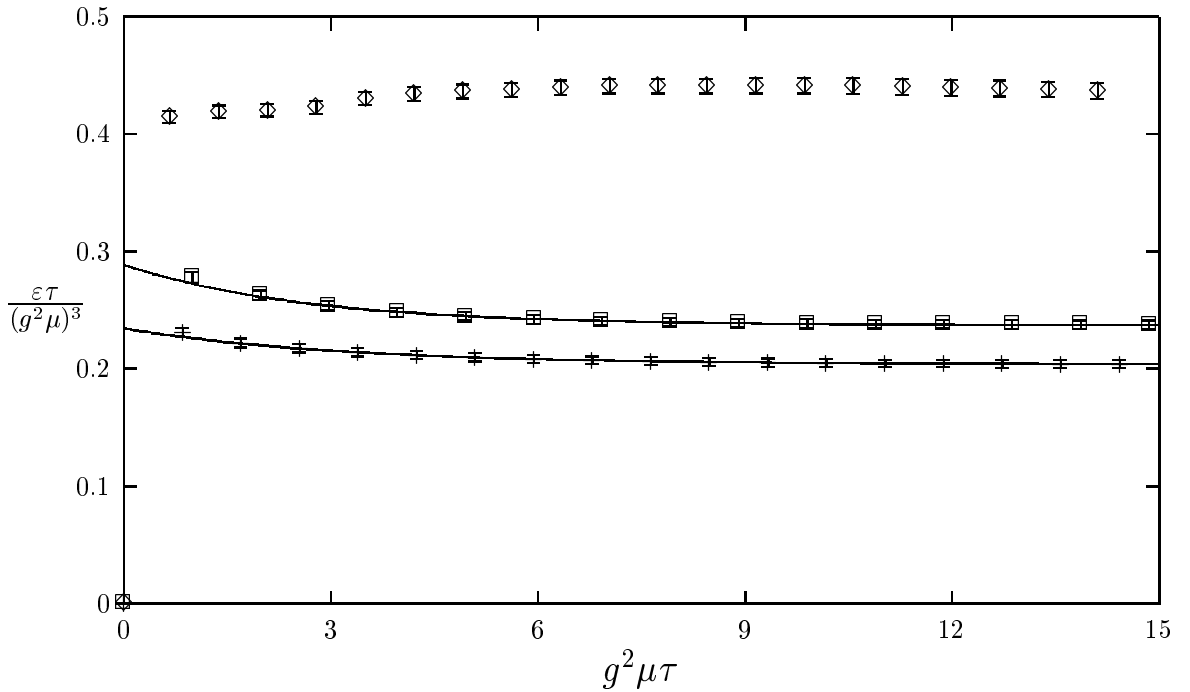


Figure 5:  $\varepsilon\tau/(g^2\mu)^3$  as a function of  $g^2\mu\tau$  for  $g^2\mu L = 5.66$  (diamonds), 35.36 (pluses) and 296.98 (squares). Both axes are in dimensionless units. Note that  $\varepsilon\tau = 0$  at  $\tau = 0$  for all  $g^2\mu L$ . The lines are exponential fits  $\alpha + \beta e^{-\gamma\tau}$  including all points beyond the peak.

quantity  $\varepsilon\tau$  has the physical interpretation of the energy density of produced gluons



$dE/L^2/d\eta$  only at late times—when  $\tau \sim t$ . Though  $\varepsilon\tau$  goes to a constant in all three cases, the approach to the asymptotic value is different. For the smallest  $g^2\mu L$ ,  $\varepsilon\tau$  increases continuously before saturating at late times. For larger values of  $g^2\mu L$ ,  $\varepsilon\tau$  increases rapidly, develops a transient peak at  $\tau \sim 1/g^2\mu$ , and decays exponentially there onwards, satisfying the relation  $\alpha + \beta e^{-\gamma\tau}$ , to a constant value  $\alpha$  (equal to the lattice  $dE/L^2/d\eta$ ). The lines shown in the figure are from an exponential fit including all the points past the peak. This behavior is satisfied for all  $g^2\mu L \geq 8.84$ , independently of  $N$ .

Given the excellent exponential fit, one can interpret the decay time  $\tau_D = 1/\gamma/g^2\mu$  as the appropriate scale controlling the formation of gluons with a physically well defined energy. In other words,  $\tau_D$  is the “formation time” in the sense used by Bjorken [55]. In Table 1, we tabulate  $\gamma$  versus  $g^2\mu L$  for the largest  $N \times N$  lattices for all but the smallest  $g^2\mu L$ . For large  $g^2\mu L$ , the formation time decreases with increasing  $g^2\mu L$ , as we expect it should. The reason the smallest value of  $g^2\mu L$  does not have a transient peak is likely because in this case the  $k_t$  modes do not sufficiently sample the region  $k_t \leq Q_s$  where non-linearities are important. The few modes there are, lie in the perturbative region where the fields can be linearized at  $\tau = 0$ .

The physical energy per unit area per unit rapidity of produced gluons can be defined in terms of a function  $f(g^2\mu L)$  as

$$\frac{1}{L^2} \frac{dE}{d\eta} = \frac{1}{g^2} f(g^2\mu L) (g^2\mu)^3. \quad (70)$$

As discussed in Ref. [21], the function  $f$  is obtained for each fixed value of  $g^2\mu L$ , by taking the continuum limit, i.e., extrapolating  $g^2\mu a \rightarrow 0$ . In Fig. 6, we plot the striking behavior of  $f$  with  $g^2\mu L$ . For very small  $g^2\mu L$ 's, it changes very slightly but then changes rapidly by a factor of two from 0.427 to 0.208 when  $g^2\mu L$  is changed from 8.84 to 35.36. From 35.36 to 296.98, nearly an order of magnitude in  $g^2\mu L$ , it changes by  $\sim 25\%$ . The precise values of  $f$  and the errors are tabulated in Table 1.

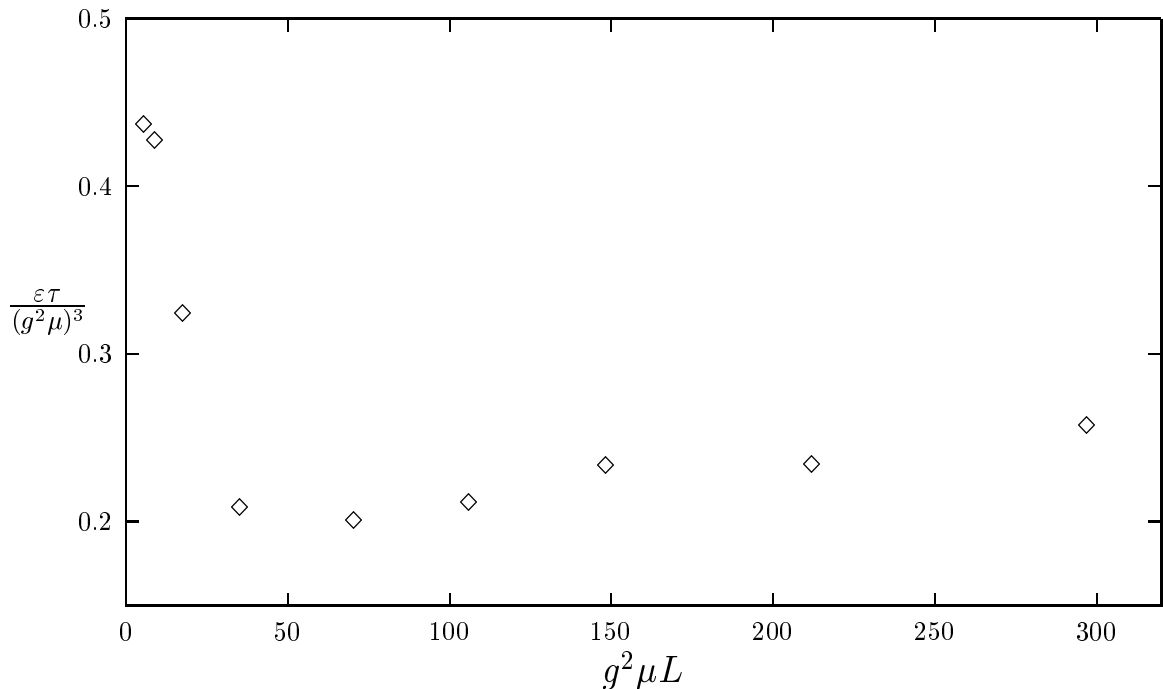


Figure 6:  $\varepsilon\tau/(g^2\mu)^3$  extrapolated to the continuum limit:  $f$  as a function of  $g^2\mu L$ . The error bars are smaller than the plotting symbols.

What is responsible for the dramatic change in the behavior of  $f$  as a function of  $g^2\mu L$ ? In  $A^\tau = 0$  gauge, the dynamical evolution of the gauge fields depends entirely on the initial conditions, namely, the parton distributions in the wavefunctions of the incoming nuclei [56]. In the nuclear wavefunction, at small  $x$ , non-perturbative, albeit weak coupling, effects become important for transverse momenta  $Q_s \sim 6\alpha_s\mu$ . Now on the lattice,  $p_t$  is defined to be  $2\pi n/L$ , where  $n$  labels the momentum mode. The condition that momenta in the wavefunctions of the incoming nuclei have saturated,  $p_t \sim 6\alpha_s\mu$ , translates roughly into the requirement that  $g^2\mu L \geq 13$  for  $n = 1$ . Thus for  $g^2\mu L = 13$ , one is only beginning to sample those modes. Indeed, this is the region in  $g^2\mu L$  in which one sees the rapid change in  $f$ . The rapid de-

$g^2\mu L$	5.66	8.84	17.68	35.36	70.7
$f$	$.436 \pm .007$	$.427 \pm .004$	$.323 \pm .004$	$.208 \pm .004$	$.200 \pm .005$
$\gamma$		$.101 \pm .024$	$.232 \pm .046$	$.165 \pm .013$	$.275 \pm .011$
$g^2\mu L$	106.06	148.49	212.13	296.98	
$f$	$.211 \pm .001$	$.232 \pm .001$	$.234 \pm .002$	$.257 \pm .005$	
$\gamma$	$.322 \pm .012$	$.362 \pm .023$	$.375 \pm .038$	$.378 \pm .053$	

Table 1: The function  $f = dE/L^2/d\eta$  and the relaxation rate  $\gamma = 1/\tau_D/g^2\mu$  tabulated as a function of  $g^2\mu L$ .  $\gamma$  has no entry for the smallest  $g^2\mu L$  since there  $\varepsilon\tau/(g^2\mu)^3$  vs  $g^2\mu\tau$  differs qualitatively from the other  $g^2\mu L$  values.

crease in  $f$  is likely because the first non-perturbative corrections are large, and have a negative sign relative to the leading term. Understanding the later slow rise and apparent saturation with  $g^2\mu L$  requires a better understanding of the number and energy distributions with  $p_t$ . This work is in progress and will be reported on separately [53].

Our results are consistent with an estimate by A. H. Mueller [57] for the number of produced gluons per unit area per unit rapidity. He obtains  $dN/L^2/d\eta = c(N_c^2 - 1)Q_s^2/4\pi^2\alpha_S N_c$ , and argues that the number  $c$  is a non-perturbative constant of order unity. If most of the gluons have  $p_t \sim Q_s$ , then  $dE/L^2/d\eta = c'(N_c^2 - 1)Q_s^3/4\pi^2\alpha_S N_c$  which is of the same form as our Eq. 70. In the  $g^2\mu L$  region of interest, our function  $f \approx 0.23$ – $0.26$ . Using the appropriate relation between  $Q_s$  and  $g^2\mu$ , we obtain  $c' = 4.3$ – $4.9$ . Since one expects a distribution in momenta about  $Q_s$ , it is very likely that  $c'$  is at least a factor of 2 greater than  $c$ —thereby yielding a number of order unity for  $c$  as estimated by Mueller. This coefficient can be determined more precisely when we compute the non-perturbative number and energy distributions.

We will now estimate the initial energy per unit rapidity of produced gluons at

RHIC and LHC energies. We do so by extrapolating from our SU(2) results to SU(3) assuming the  $N_c$  dependence to be  $(N_c^2 - 1)/N_c$  as in Mueller's formula. At late times, the energy density is  $\varepsilon = (g^2\mu)^4 f(g^2\mu L) \gamma(g^2\mu L)/g^2$ , where the formation time is  $\tau_D = 1/\gamma(g^2\mu L)/g^2\mu$  as discussed earlier. We find that  $\varepsilon^{RHIC} \approx 66.49$  GeV/fm<sup>3</sup> and  $\varepsilon^{LHC} \approx 1315.56$  GeV/fm<sup>3</sup>. Multiplying these numbers by the initial volumes at the formation time  $\tau_D$ , we obtain the classical Yang–Mills estimate for the initial energies per unit rapidity  $E_T$  to be  $E_T^{RHIC} \approx 2703$  GeV and  $E_T^{LHC} \approx 24572$  GeV respectively.

We have compared these numbers to results presented recently [58] for the mini-jet energy (computed for  $p_t > p_{sat}$ , where  $p_{sat}$  is a saturation scale akin to  $Q_s$ ). He obtains  $E_T^{RHIC} = 2500$  GeV and  $E_T^{LHC} = 12000$ . The remarkable closeness between our results for RHIC is very likely a coincidence. The Finnish groups results include  $K$  factor estimates range from 1.5–2.5. If we pick a recent value of  $K \approx 2$  [59], we obtain as our final estimate,  $E_T^{RHIC} \approx 5406$  GeV and  $E_T^{LHC} \approx 49144$  GeV.

To summarize, we discussed in this section a non-perturbative, numerical computation, for a SU(2) gauge theory, of the initial energy, per unit rapidity, of gluons produced in very high energy nuclear collisions. Extrapolating our results to SU(3), we estimated the initial energy per unit rapidity at RHIC and LHC. We plan to improve our estimates by performing our numerical analysis for SU(3). Moreover, computations in progress to determine the energy and number distributions should enable us to match our results at large transverse momenta to mini-jet calculations [53].

## 7 Summary

In these lectures, we have discussed a classical effective field theory approach to scattering at very high energies. At these energies, a saturation scale  $Q_s(x)$  controls the dynamics of high energy scattering. How this scale changes as we go to small  $x$

is described by a non-linear renormalization group equation [15, 36]. The solutions of the RG equations and the inclusion of effects such as the running of the coupling in the regime of strong non-linear fields need to be better understood. In particular, one would like to investigate possibly striking experimental signatures of this regime. Since  $Q_s(x) \gg \Lambda_{QCD}$ , weak coupling methods may be applicable. In these lectures we have shown how one may begin to apply these weak coupling methods to study DIS and high energy scattering.

## Acknowledgements

These lectures summarize work done in collaboration with Alex Krasnitz and Larry McLerran. I would like to thank Michal Praszalowicz and the other organizers of the Zakopane School for their very kind hospitality. This work was supported by the Director, Office of Energy Research, Division of Nuclear Physics of the Office of High Energy and Nuclear Physics of the US Department of Energy under contract number DOE-FG02-93-ER-40764.

## References

- [1] A. H. Mueller, *Phys. Lett.* **B396** (1997) 251.
- [2] V. N. Gribov and L. N. Lipatov, *Sov. J. Nucl. Phys.* **15** (1972) 78; G. Altarelli and G. Parisi, *Nucl. Phys.* **B126** 298 (1977); Yu. L. Dokshitzer, *Sov. Phys. JETP* **73** (1977) 1216.
- [3] E. Laenen and E. M. Levin, *Ann. Rev. Nucl. Part. Sci.* **44** (1994) 199; E. M. Levin, *Heavy Ion Phys.* **8**265 (1998).
- [4] L. Frankfurt, W. Koepf and M. Strikman, *Phys. Rev.* **D54** (1996) 3194; L. Frankfurt and M. Strikman, hep-ph/9806536.

- [5] L. N. Lipatov, *Phys. Rept.* **286** (1997) 131.
- [6] E. A. Kuraev, L. N. Lipatov and V. S. Fadin, *Sov. Phys. JETP* **45**, 199 (1977);  
Ya. Ya. Balitsky and L. N. Lipatov, *Sov. J. Nucl. Phys.* **28** (1978) 22.
- [7] I. Abt et al., *Nucl. Phys.* **B407** (1993) 515; M. Derrick et al., *Z. Phys.* **C72**  
(1996) 399.
- [8] M. Gluck, E. Reya and A. Vogt, *Z. Phys.* **C67** (1995) 433; hep-ph/9806404;  
H. L. Lai et al., *Phys. Rev.* **D55** (1997) 1280.
- [9] V. S. Fadin and L. N. Lipatov, hep-ph/9802290; G. Camici and M. Ciafaloni,  
*Phys. Lett.* **B412** (1997) 396; Erratum-ibid., **B417** (1998) 390; Y. V.  
Kovchegov and A. H. Mueller, *Phys. Lett.* **B439** 428 (1998).
- [10] Gavin Salam, *these proceedings*.
- [11] L. McLerran and R. Venugopalan, *Phys. Rev.* **D49** (1994) 2233; **D49** (1994)  
3352.
- [12] A. Ayala, J. Jalilian–Marian, L. McLerran and R. Venugopalan, *Phys. Rev.* **D52**  
(1995) 2935; *ibid.* **D53** (1996) 458.
- [13] J. Jalilian–Marian, A. Kovner, L. McLerran and H. Weigert, *Phys. Rev.* **D55**  
(1997) 5414.
- [14] J. Jalilian–Marian, A. Kovner, A. Leonidov and H. Weigert, *Nucl. Phys.* **B504**  
(1997) 415.
- [15] J. Jalilian–Marian, A. Kovner and H. Weigert, hep-ph/9709432.
- [16] J. Jalilian–Marian, A. Kovner, A. Leonidov and H. Weigert, hep-ph/9807462;  
E. Iancu, A. Leonidov and L. McLerran, in progress.
- [17] L. McLerran and R. Venugopalan, *Phys. Lett* **B 424** (1998) 15.

- [18] L. McLerran and R. Venugopalan, *Phys. Rev.* **D59** (1999) 094002.
- [19] A. Krasnitz and R. Venugopalan, hep-ph/9706329, hep-ph/9808332.
- [20] A. Krasnitz and R. Venugopalan, *Nucl. Phys.* **B557** (1999) 237.
- [21] A. Krasnitz and R. Venugopalan, hep-ph/9909203.
- [22] L. McLerran, *these proceedings*.
- [23] Yuri V. Kovchegov, *Phys. Rev.* **D54** (1996) 5463; **D55** (1997) 5445.
- [24] A. H. Mueller, hep-ph/9904404.
- [25] C. S. Lam and G. Mahlon, hep-ph/9907281; G. Mahlon, hep-ph/9907285.
- [26] S. Pokorski, *Gauge field theories*, Cambridge Univ. Press, (1987).
- [27] J. Kogut and D. Soper, *Phys. Rev.* **D1** (1970) 2901; J. Bjorken, J. Kogut and D. Soper, *Phys. Rev.* **D3** (1971) 1382.
- [28] R. L. Jaffe, *Nucl. Phys.* **B229** (1983) 205.
- [29] L. McLerran and R. Venugopalan, *Phys. Rev.* **D50** (1994) 2225.
- [30] A. Hebecker and H. Weigert, *Phys. Lett.* **B432** 215 (1998).
- [31] I. Balitsky, *Phys. Rev.* **D60** 014020 (1999); *Phys. Rev. Lett.* **81** 2024 (1998).
- [32] N. N. Nikolaev and B. G. Zakharov, *Z. Phys.* **C49** (1991) 607.
- [33] J. Breitwig et al. (ZEUS collaboration) *Eur.Phys. J.* **C7** (1999) 609.
- [34] E. Gotsman, E. Levin, U. Maor, and E. Naftali, *Nucl. Phys.* **B539**, 535 (1999); *Phys. Lett.* **B425** (1998) 36; K. Golec-Biernat, M. Wüsthoff, *Phys. Rev.* **D59**, 014017 (1999); A.L. Ayala Filho, M.B. Gay Ducati, and E.M. Levin *Eur.Phys.J.* **C8115** (1999). A. L. Ayala Filho, M. B. Gay Ducati, and V. P. Gonsalves, *Phys. Rev.* **D59** 054010 (1999).

- [35] A. H. Mueller, *Nucl. Phys.* **B307** (1988) 34; **B317** (1989) 573; **B335** (1990) 115.
- [36] Yuri V. Kovchegov, hep-ph/9905214.
- [37] E. M. Levin and K. Tuchin, hep-ph/9908317.
- [38] G. G. Callan and D. J. Gross, *Phys. Rev. Lett.* **22** (1969) 156.
- [39] A. Zee, F. Wilczek and S. B. Treiman, *Phys. Rev.* **D10** (1974)2881.
- [40] W. Bardeen, A. J. Buras, D. W. Duke and T. Muta, *Phys. Rev.* (1978) 3998.
- [41] M. Gyulassy and L. McLerran, *Phys. Rev.* **C56** (1997) 2219.
- [42] A. Kovner, L. McLerran and H. Weigert, *Phys. Rev* **D52** 3809 (1995); **D52** 6231 (1995).
- [43] J. F. Gunion and G. Bertsch, *Phys. Rev.* **D25** (1982) 746.
- [44] Yuri Kovchegov and Dirk Rischke, *Phys. Rev.* **C56** 1084 (1997).
- [45] S. G. Matinyan, B. Müller and D. H. Rischke, *Phys. Rev.* **C56** (1997) 2191; *Phys. Rev.* **C57** (1998) 1927.
- [46] Xiao-feng Guo, *Phys. Rev.* **D59** 094017 (1999).
- [47] K. Kajantie, P. V. Landshoff, and J. Lindfors, *Phys. Rev. Lett.* **59** (1987) 2527; K. J. Eskola, K. Kajantie, and J. Lindfors, *Nucl. Phys.* **323** (1989) 37; J.-P. Blaizot and A. H. Mueller, *Nucl. Phys. B289* 847 (1987).
- [48] A. H. Mueller, hep-ph/9909388; hep-ph/9906322.
- [49] M. Gyulassy and X.-N. Wang, *Nucl. Phys.* **420** (1994) 583.
- [50] K. J. Eskola, B. Müller, and X.-N. Wang, *Phys. Lett.* **B374** (1996) 20.



- [51] A. Makhlin, hep-ph/9608261.
- [52] J. Kogut and L. Susskind, *Phys. Rev.* **D11** 395 (1975).
- [53] A. Krasnitz and R. Venugopalan, in progress.
- [54] R. V. Gavai and R. Venugopalan, *Phys. Rev.* **D54** 5795 (1996).
- [55] J. D. Bjorken, *Phys.Rev.* **D27** 140 (1983).
- [56] Y. V. Kovchegov and A. H. Mueller *Nucl. Phys.* **B529** 451 (1998).
- [57] A. H. Mueller, hep-ph/9906322.
- [58] K. J. Eskola, K. Kajantie, P. V. Ruuskanen, and K. Tuominen, hep-ph/9909456; K. Kajantie, hep-ph/9907544; K. J. Eskola and K. Kajantie, *Z. Phys.* **C75** 515 (1997).
- [59] A. Leonidov and D. Ostrovsky, hep-ph/9811417.